


# Magnetic band representations, Fu-Kane-like symmetry indicators, and magnetic topological materials

Jiacheng Gao, Zhaopeng Guo, Hongming Weng, and Zhijun Wang <sup>\*</sup>

*Beijing National Laboratory for Condensed Matter Physics, and Institute of Physics, Chinese Academy of Sciences, Beijing 100190, China and University of Chinese Academy of Sciences, Beijing 100049, China*



(Received 24 April 2022; accepted 12 July 2022; published 28 July 2022)

To realize novel topological phases and to pursue potential applications in low-energy consumption spintronics, the study of magnetic topological materials is of great interest. Starting from the theory of nonmagnetic topological quantum chemistry [Bradlyn *et al.*, *Nature* **547**, 298 (2017)], we have obtained irreducible (co)representations and compatibility relations (CRs) in momentum space, and we constructed a complete list of magnetic band (co)representations (MBRs) in real space for other magnetic space groups (MSGs) with antiunitary symmetries (i.e., type-III and type-IV MSGs). The results are consistent with the magnetic topological quantum chemistry [Elcoro *et al.*, *Nat. Commun.* **12**, 5965 (2021)]. Using the CRs and MBRs, we reproduce the symmetry-based classifications for MSGs, and we obtain a set of Fu-Kane-like formulas of symmetry indicators (SIs) in both spinless (bosonic) and spinful (fermionic) systems, which are implemented in an automatic code—TOPMAT—to diagnose topological magnetic materials. The magnetic topological materials, whose occupied states cannot be decomposed into a sum of MBRs, are consistent with nonzero SIs. Lastly, using our online code, we have performed spin-polarized calculations for magnetic compounds in the materials database, and we find many magnetic topological candidates.

DOI: [10.1103/PhysRevB.106.035150](https://doi.org/10.1103/PhysRevB.106.035150)

## I. INTRODUCTION

In the past few decades, the topological phases of matter have attracted a great deal of interest in the field of condensed-matter physics. New phenomena such as the integer and fractional quantum Hall effects [1–3], time-reversal invariant two- and three-dimensional topological insulators (TIs) [4–8], topological crystalline insulators (TCIs) [9–14], and topological semimetals [15–20] have been discovered. The topologically nontrivial materials exhibit robust transport properties such as the quantized Hall and magnetoelectric effects, surface states, and Fermi arcs. Theoretical works reveal that the topology of noninteracting electrons in three-dimensional (3D) crystals relies on the structure of Bloch states as a function of momentum. Most recently, the symmetry eigenvalues or irreducible representations (irreps) of all 230 space groups were used to characterize topological materials through the theories of symmetry-based indicators [21–24] and topological quantum chemistry (TQC) [25]. As a result, high-throughput screening for topological materials has been performed in nonmagnetic materials [26–28].

Previous studies [21,23,25,29] have concentrated on nonmagnetic space groups, which are known as 230 type-II magnetic space groups (MSGs) with time reversal ( $\mathcal{T}$ ). In fact, there are 1651 MSGs, each of which generally contains a unitary part and an antiunitary part ( $\mathbf{M} \equiv \mathbf{G} + A\mathbf{G}$ , where  $\mathbf{M}$  is a MSG,  $\mathbf{G}$  is its unitary part, and  $A$  is an antiunitary symmetry).

These MSGs can also be categorized into four classes: 230 ordinary crystallographic space groups without any antiunitary symmetry (type I with  $A = \emptyset$ ), 230 type-II (with  $A = \mathcal{T}$ ), 674 type-III, and 517 type-IV groups (with  $A = \mathcal{TR}$ ). In the type-IV group,  $R$  is a pure translation, and other cases belong to the type-III group. In the nonmagnetic TQC work, the irreps and compatibility relations (CRs) in momentum space and the (elementary) band representations (BRs) are enumerated for type-I and type-II MSGs. To extend the TQC theory to all MSGs, the enumerations of irreducible corepresentations (coirreps), CRs and MBRs, for the type-III and type-IV MSGs are needed. Even though the symmetry-based classifications of all MSGs were finished in Ref. [30], they do not give the physical meaning of the symmetry indicators (SIs). Recently, the authors of Refs. [31,32] developed magnetic topological quantum chemistry (MTQC) and obtained physically meaningful SIs for MSGs. They released the full set of MTQC, including the corepresentations, their compatibility relations, and the magnetic band corepresentations accordingly [32]. On the other hand, the mappings from SIs to topological invariants in MSGs have also been investigated in Refs. [33–35].

In this work, starting from the CRs and BRs of the nonmagnetic TQC, we have reconstructed MBRs and the Fu-Kane-like formulas of SIs for MSGs. Although they were obtained in the MTQC during the long preparation of this work, it is important to have independent works to generate them and apply them in the DFT calculations due to the complexity of the problem. Therefore, we have developed an automatic code—TOPMAT [36]—to diagnose magnetic topological materials, and we performed a theoretical search for

<sup>\*</sup>wzj@iphy.ac.cn

topological magnetic materials. In Sec. II, we review non-magnetic TQC theory in type-I (and type-II with  $\mathcal{T}$ ) MSGs, and then we derive coirreps, CRs, and MBRs of type-III and type-IV MSGs. In Sec. III, we reproduce the symmetry-based classifications for MSGs, and we obtain the Fu-Kane-like formulas of SIs by Smith decomposition. An online code—TOPMAT—is developed to compute them for any (non)magnetic material with the input “tqc.data” (from IRVSP) [37]. Finally, in Sec. IV, based on spin-polarized density functional theory (DFT) calculations, we have performed a theoretical search for topological magnetic compounds in the materials database by using our homemade codes. Some good candidates are presented.

## II. MTQC IN 1651 MSGs

In topologically trivial band structures, the Wannier functions are exponentially localized and respect the crystal symmetries. A set of bands arising from localized, symmetric Wannier functions form a representation of the crystal symmetry group, and they are referred to as BR in TQC theory. TQC theory contains two concrete aspects. (i) The CRs: based on them, one can get the information of irreps at any  $k$ -points in the entire Brillouin zone (BZ) from those at maximal high-symmetry  $k$ -points (HSKPs) only, which makes it possible for the high-throughput screening for topological materials. (ii) A full list of (elementary) BRs: they are given by not only the irreps in momentum space, but also by a specific set of orbitals (i.e.,  $\rho@q$ ) in real space. The materials, whose occupied states cannot be expressed as a sum of BRs, are classified to be topological. On the other hand, these BRs also indicate the orbital character in real space, i.e., the average charge center and site-symmetry character. Therefore, the application of TQC has allowed for the discovery of both topologically nontrivial materials with novel phenomena [26–28,31] and topologically trivial unconventional materials (or obstructed atomic limits) with interesting properties [38–41].

### A. TQC in MSGs without antiunitary symmetry

The CRs in momentum space and the BRs in real space are obtained and established for 230 type-I MSGs in Refs. [25,42,43]. We briefly review space-group operators, assuming the reader is a physicist familiar with group theory. In 3D crystals, space-group operators,  $h \equiv \{R_h|\mathbf{v}_h\}$ , consist of two parts: a rotation part  $R_h$  and a translation part  $\mathbf{v}_h$ . The product of two operations is defined as  $\{R_s|\mathbf{v}_s\}\{R_t|\mathbf{v}_t\} = \{R_s R_t | R_s \mathbf{v}_t + \mathbf{v}_s\}$ . The lattice translation  $\{E|\mathbf{L}\}$  acting on a Bloch state  $\phi_{\mathbf{k}}$  gives a phase factor of  $e^{-i\mathbf{k}\cdot\mathbf{L}}$ .

#### 1. Compatibility relations in momentum space

We start by identifying the maximal  $k$ -vectors in the first BZ [44,45]. The little group of  $\mathbf{k}$  is defined as  $LG(\mathbf{k}) : \{h|h\mathbf{k} = \mathbf{k} + \mathbf{B}, h \in \mathbf{G}\}$  with  $\mathbf{B}$  integer reciprocal-lattice translations. In a 3D BZ, all adjacent  $\mathbf{k}_i$  points connecting to the maximal  $k$ -vector  $\mathbf{k}_0$  satisfy  $LG(\mathbf{k}_i) \subset LG(\mathbf{k}_0)$ . The group theory tells us that the irreducible representation of  $LG(\mathbf{k}_0)$  is also a representation of  $LG(\mathbf{k}_i)$ , which may be reducible or not. These relations are known as the CRs [42].

### 2. Band representations in real space

For any position  $\mathbf{q}$  in the unit cell of a crystal, the set of symmetry operations  $s \in \mathbf{G}$  that leave  $\mathbf{q}$  fixed (absolutely, not up to integer lattice translations  $\mathbf{L}$ ) is called the stabilizer group, or the site-symmetry group  $G_{\mathbf{q}}$ . By definition, a site-symmetry group is isomorphic to a point group. Thus, we assume that the local orbits  $|W_j(\vec{r} - \mathbf{q})\rangle$  ( $j = 1, \dots, m$ ) are transformed as a basis of the  $m$ -dimensional representation  $\rho$  [i.e.,  $\Delta^\rho(s)$  is the  $m \times m$  matrix representation of symmetry operation  $s$  in irrep  $\rho$ ].

The set of positions  $\{\mathbf{q}_\alpha = g_\alpha \mathbf{q} | \mathbf{q}_\alpha \neq \mathbf{q}_\beta + \mathbf{L}\}$ ;  $g_1 = \{E|000\}$ ;  $\alpha, \beta = 1, \dots, n$  are classified by a Wyckoff position of multiplicity  $n$ . Thus, one can find that there are  $m \times n$  orbitals  $|W_j^\alpha(\vec{r} - \mathbf{q}_\alpha)\rangle \equiv |g_\alpha W_j(\vec{r} - \mathbf{q})\rangle$  in a unit cell. Considering the duplicates due to the lattice translations, the space group  $\mathbf{G}$  is spanned by the set of all the orbitals ( $\rho@q$ ). In other words, they form a representation of  $\mathbf{G}$  in real space. After Fourier transforms, we can derive the corresponding matrix representation of symmetry operation  $h$  (at any  $k$ ) as follows:

$$\begin{aligned} c_{\mathbf{k},j\alpha}^\dagger : a_{\mathbf{k},j\alpha}(\vec{r}) &= \frac{1}{\sqrt{N}} \sum_{\mathbf{L}} e^{i\mathbf{k}\cdot(\mathbf{q}_\alpha + \mathbf{L})} W_j^\alpha(\vec{r} - \mathbf{q}_\alpha - \mathbf{L}), \\ hc_{\mathbf{k},j\alpha}^\dagger &= e^{-i(h\mathbf{k})\cdot\mathbf{L}_{\beta\alpha}} \sum_{j'} \Delta_{j'j}^\rho(s) c_{R_h \mathbf{k},j'\beta}^\dagger \\ &\text{with } s = g_\beta^{-1} \{E | -\mathbf{L}_{\beta\alpha}\} h g_\alpha. \end{aligned} \quad (1)$$

Here,  $\beta$  and  $\mathbf{L}_{\beta\alpha}$  are determined by  $h\mathbf{q}_\alpha \equiv \mathbf{q}_\beta + \mathbf{L}_{\beta\alpha}$ . Thus, the matrix representations of  $\mathbf{G}$  are given in Eq. (1) on the basis of  $\{|a_{\mathbf{k},j\alpha}(\vec{r})\rangle, |a_{\mathbf{k}_2,j\alpha}(\vec{r})\rangle, \dots, |a_{\mathbf{k}_l,j\alpha}(\vec{r})\rangle\}$  with  $j = 1, \dots, m$  and  $\alpha = 1, \dots, n$ . The set of symmetry-related  $k$ -vectors  $\{\mathbf{k}_\gamma = R_{h_\gamma} \mathbf{k} | \mathbf{k}_\gamma \neq \mathbf{k}_\delta + \mathbf{B}\}$ ;  $h_1 = \{E|000\}$ ;  $\gamma, \delta = 1, \dots, l$  are classified by  $k$ -stars. The little group of  $LG(\mathbf{k})$  is presented in the basis of  $\{|a_{\mathbf{k},j\alpha}(\vec{r})\rangle\}$ . By assigning the representations to the irreps of the  $k$  little group [43], one can obtain a set of  $k$ -irreps of the BR  $\rho@q$ , especially at the maximal  $k$ -vectors.

### B. TQC in MSGs with antiunitary symmetry

To construct BRs in MSGs with antiunitary symmetry (AS), one needs to get the relations between coirreps in momentum space and AS-related orbitals in real space. To get an appropriate description of a MSG  $\mathbf{M}$ , one should start with its unitary group  $\mathbf{G}$ . Saying the eigenstates  $|\phi_{j=1,\dots,m}\rangle$  transform as an  $m$ -dimensional irrep  $\rho$  of  $\mathbf{G}$ , one can take  $|\phi_j\rangle$  and  $A|\phi_j\rangle$  as the bases for the magnetic group  $\mathbf{M}$ . Thus, these bases are dubbed “corepresentations” of  $\mathbf{M}$ , denoted as  $D$  below. To analyze the reducibility of a corepresentation of a MSG, one can apply the “Herring rule” [46–48],

$$\frac{1}{|\mathbf{G}|} \sum_{B \in \mathbf{AG}} \chi_\rho(B^2) = \begin{cases} 1 & \text{case (a),} \\ -1 & \text{case (b),} \\ 0 & \text{case (c),} \end{cases} \quad (2)$$

where  $\chi_\rho$  is the character of irrep  $\rho$ , and  $|\mathbf{G}|$  is the number of elements in  $\mathbf{G}$ . The Herring rule classifies  $\rho$  into three classes:  $\rho^{(a)}$ ,  $\rho^{(b)}$ , and  $\rho^{(c)}$ . In case (a), the corepresentation  $D$  is reducible,  $D = \rho_i^{(a)} \oplus \rho_i^{(a)}$ , while in cases (b) and (c),  $D$  is irreducible, resulting in the double degeneracy of  $\rho_i^{(b)}$ ,  $\rho_i^{(c)}$ .

and  $\rho_i^{(c)}\rho_j^{(c)}$ , respectively. Two related irreps of case (c) are satisfied in the condition  $[\chi_{\rho_i}(R) \equiv \chi_{\rho_i}^*(A^{-1}RA)]$ . Thus, the coirreps of the magnetic group  $\mathbf{M}$  are labeled by the combined irreps of unitary group  $\mathbf{G}$ :  $\rho_i^{(a)}$ ,  $\rho_i^{(b)}$ ,  $\rho_i^{(b)}$ , and  $\rho_i^{(c)}\rho_j^{(c)}$ .

### 1. Irreducible corepresentations in momentum space

First, we need to identify its unitary group  $\mathbf{G}$ . After considering the Herring rule in Eq. (2), we can label all the coirreps of  $\mathbf{M}$  by the combined irreps of  $\mathbf{G}$ . In this work, all the coirreps for MSGs are solved. They are presented explicitly in the Supplemental Material (SM) [49]. Thus, from the CRs of type-I MSG obtained in the previous work [25], the CRs for coirreps in type-III and type-IV MSG can be conveniently worked out. To calculate the corresponding coirreps in the DFT calculations, the unitary group of a MSG is crucial, which can be obtained online [50] (see the MSG tables in the SM [49]). With the program IRVSP and its unitary group, one can get the coirreps for a magnetic compound.

### 2. Magnetic band representations in real space

At a magnetic Wyckoff position  $\mathbf{q}$  in a MSG [51], if its site-symmetry group is antiunitary, we have to figure out the degeneracy of the irreps of its unitary part by the Herring rule in Eq. (2) (isomorphic to magnetic point groups). Otherwise, we have to add other AS-related orbitals to form a MBR in real space. Thus, we can get the MBRs for MSGs from the BRs of type-I MSGs. After solving the matching of the orbitals in real space, MBRs are obtained and presented explicitly in the SM [49].

## III. SYMMETRY-BASED INDICATORS OF MSGs

With the CRs and coirreps for all MSGs, a MBR can be expressed as a vector, consisting of the numbers of different coirreps at maximal HSKPs. They form a vector space {BR} in which the linearly independent ones are regarded as elementary (M)BRs. On the other hand, the coirreps of band structures, satisfying the CRs, form another vector space

{CR}. These band structures can be classified by the quotient group of  $\frac{\{\text{CR}\}}{\{\text{BR}\}}$  [21]. We derive the symmetry-based classifications of MSGs by Smith decomposition [52,53], which are consistent with Refs. [30–32]. The Fu-Kane-like formulas of the SIs are obtained in the tables of the SM [49] and computed by an online code (TOPMAT) for any magnetic material.

The occupied bands of a material can also be expressed as a vector. If it is a sum of BRs, it is consistent with the trivial case with zero SIs. Otherwise, it is topological with nonzero SIs. In fact, the BR decomposition approach is equivalent to the SI description. Unlike the symmetry-based classifications for type-II MSG, the classifications of other MSGs may yield a Weyl semimetal phase. For example, an odd-number inversion-based  $z_4$  and an odd-number  $S_4$ -based  $z_2$  indicate a set of Weyl nodes at some generic momenta [54–56]. For more information, one can find the physically meaningful SIs for MSGs in Refs. [31–35].

## IV. SEARCHING FOR MAGNETIC TOPOLOGICAL MATERIALS

To search for magnetic topological materials, we have performed spin-polarized DFT calculations with Hubbard- $U$  calculations (i.e.,  $U = 3$  and  $7$  eV for  $d$  and  $f$  electrons, respectively). To investigate different magnetic configurations, noncollinear magnetism and spin-orbit coupling are considered in our calculations. We propose an automatic process to search for topological magnetic materials. It is implemented in MAGTOP [36], and it is user-friendly for the DFT researchers. The searching process can be easily reproduced online by others for any magnetic material.

### A. An automatic process to search for topological materials

(i) We generate POSCAR (SG #A) of a crystallographic structure with magnetic atoms from the materials database. Then, we run PHONOPY to standardize the structure and generate PPOSCAR.

TABLE I. The table of magnetic topological candidates shows the ICSD number, magnetic space group and type, the converged energy, and the nonzero SIs.

No. ICSD	No. MSG (OG)	Type	Energy (eV/atom)	SIs
44084 SG223 V <sub>3</sub> As	1608	III	-5.9877	$z_2 = 1$
58096 SG223 V <sub>3</sub> Sb	1608	III	-5.7167	$z_2 = 1$
428795 SG164 EuMg <sub>2</sub> Bi <sub>2</sub>	1319	III	-4.9684	$z_2 = 0, z_{12} = 9$
	1321	IV	-4.9687	$z_2 = 1$
67671 SG194 InMnO <sub>3</sub>	1497	III	-6.5824	$z_3 = 2$
	1501	III	-6.5832	$z_3 = 0, z_6 = 4$
260109 SG194 EuIn <sub>2</sub> As <sub>2</sub>	1499	III	-5.5771	$z_2 = 1$
	1501	III	-5.5768	$z_3 = 2, z_6 = 3$
97965 SG148 La <sub>2</sub> CuRuO <sub>6</sub>	1247	I	-6.9781	$z_2 = 1, z_4 = 3$
104953 SG221 Mn <sub>3</sub> Pt	1600	IV	-7.1117	$z_4 = 1$
20449 SG11 YClO <sub>2</sub>	65	IV	-5.9291	$z_2 = 1$
20492 SG11 GdClO <sub>2</sub>	65	IV	-8.2142	$z_2 = 1$
76845 SG221 Mn <sub>3</sub> GaC	1600	IV	-6.5658	$z_4 = 2$
76070 SG221 Mn <sub>3</sub> ZnN	1600	IV	-6.2377	$z_4 = 2$

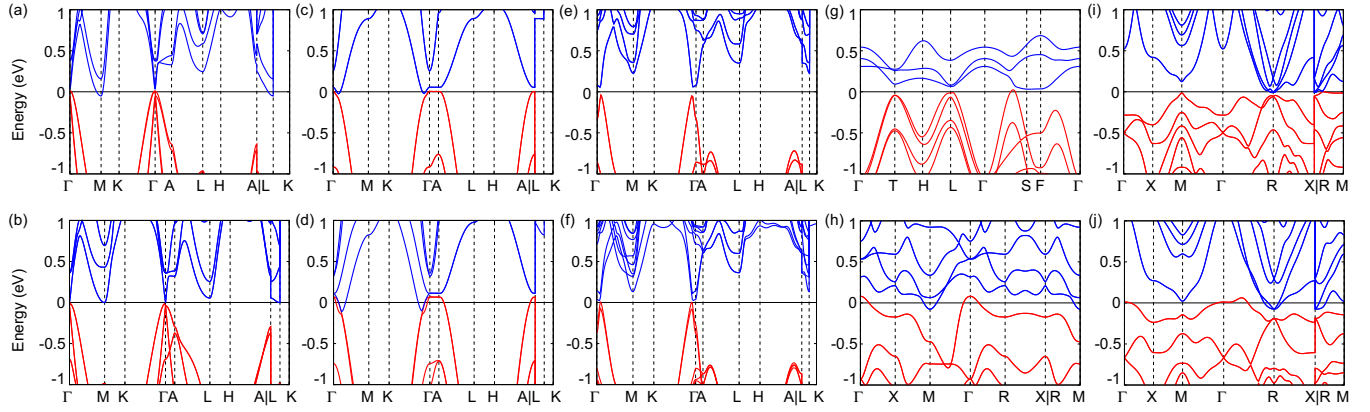


FIG. 1. Band structures of magnetic topological candidates: (a) MSG1319  $\text{EuMg}_2\text{Bi}_2$ , (b) MSG1321  $\text{EuMg}_2\text{Bi}_2$ , (c) MSG1497  $\text{InMnO}_3$ , (d) MSG1501  $\text{InMnO}_3$ , (e) MSG1499  $\text{EuIn}_2\text{As}_2$ , (f) MSG1501  $\text{EuIn}_2\text{As}_2$ , (g) MSG1247  $\text{La}_2\text{CuRuO}_6$ , (h) MSG1600  $\text{Mn}_3\text{Pt}$ , (i) MSG1608  $\text{V}_3\text{As}$ , and (j) MSG1608  $\text{V}_3\text{Sb}$ .

(ii) The MSGs in the Opechowski-Guccione (OG) setting [50] (A.1.X, A.2.X, ...) for different magnetic configurations can be generated by our code. The unitary-part group (SG #B) and the magnetic configuration in a MSG are given explicitly by TOPMAT. For compounds with local magnetic moments on magnetic atoms (neglecting type-II MSGs), we perform the DFT calculations to obtain the total energies and Bloch states on maximal HSKPs. By comparing their total energies (per atom), one can tell the ground-state configuration and metastable configurations.

(iii) By using IRVSP (irvsp -sg #B), we compute the (co)irreps for occupied bands and generate tqc.data. Then, we use the online code TOPMAT to solve the CRs and compute the SIs. One can find the Fu-Kane-like SIs in the MSG tables of the SM [49]. If the band structure does not satisfy CRs, it is a symmetry-protected magnetic metal with crossing points

near the  $E_F$ . Otherwise, it could be a topological magnetic insulator if it has nonzero SIs.

## B. Magnetic topological candidates

Based on the DFT calculations, we find some magnetic topological candidates in Table I with nonzero SIs. Their band structures are shown in Figs. 1 and 2. To understand detailed nontrivial topology, such as an antiferromagnetic topological insulator (AFM TI), an axionic insulator, and a magnetic topological crystalline insulator (MTCI), one needs to do extra work, such as the Wannier charge centers of 1D Wilson loops. In the following, we have investigated  $\text{GdClO}_2$  and  $\text{Mn}_3\text{ZnN}$  compounds in detail. Their crystal structures and magnetic configurations are generated by the workflow described in Sec. IV A.

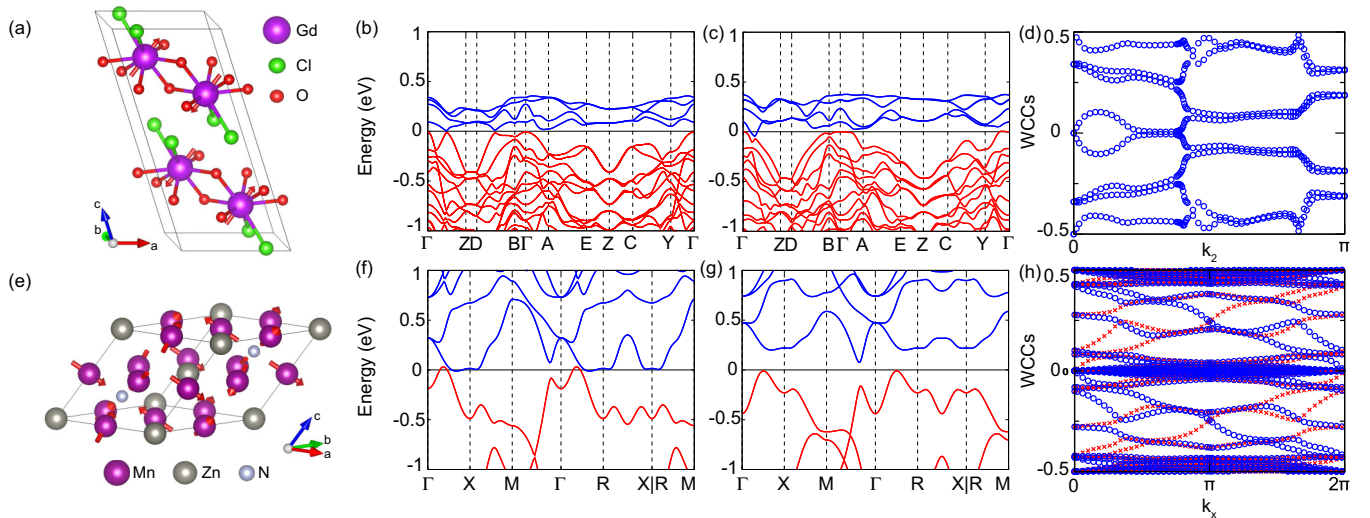


FIG. 2. Crystal structures and magnetic configurations (denoted by red arrows) of (a)  $\text{GdClO}_2$  and (e)  $\text{Mn}_3\text{ZnN}$ . Band structures of magnetic topological candidates: (b) MSG65  $\text{YClO}_2$ , (c) MSG65  $\text{GdClO}_2$ , (f) MSG1600  $\text{Mn}_3\text{GaC}$ , (g) MSG1600  $\text{Mn}_3\text{ZnN}$ . (d) WCCs of the  $k_1k_2$  plane in MSG65  $\text{GdClO}_2$ . (h) WCCs of the  $k_xk_y$  plane in MSG1600  $\text{Mn}_3\text{ZnN}$ .

The SI of MSG65 type-IV  $\text{GdClO}_2$  is computed to be  $z_2 = 1$ , indicating nontrivial nature. Its magnetic band structure is presented in Fig. 2(c). In the configuration of MSG 65 ( $P_{2c}2_1/m'$ ), the AS operator is  $\{\mathcal{T}|00\frac{1}{2}\}$ . Thus, the  $k_1k_2$  2D plane has a time-reversal  $\mathbb{Z}_2$  classification. Note that all energy bands are doubly degenerate in the bulk due to the presence of inversion symmetry  $\{\mathcal{Z}|000\}$  with the relation  $[\{\mathcal{T}|00\frac{1}{2}\}\{\mathcal{Z}|000\}]^2 = -1$ . The Wannier charge centers (WCCs) on  $k_1$ -directed Wilson loops are computed and plotted as a function of  $k_2$  in Fig. 2(d). At  $\bar{\Gamma}$  ( $k_2 = 0$ ) and  $\bar{Y}$  ( $k_2 = \pi$ ), all the WCCs are twofold, and they switch partners during the revolution, indicating  $z_2 = 1$  with nontrivial  $\mathbb{Z}_2$  topology. Thus, MSG65 type-IV  $\text{GdClO}_2$  belongs to the AFM TI phase. On the  $\{\mathcal{T}|00\frac{1}{2}\}$ -preserving (100)-surface, the topological gapless surface states are expected.

The SI of MSG1600 type-IV  $\text{Mn}_3\text{ZnN}$  is computed to be  $z_4 = 2$ . Its insulating band structure is shown in Fig. 2(g). In the magnetic configuration of MSG 1600 ( $P_Fm\bar{3}m'$ ), an AS operator is  $\{\mathcal{T}|00\frac{1}{2}\}$  [with respect to the (cubic) conventional cell of MSG structure]. A mirror symmetry  $\{m_z|000\}$  is preserved in the  $k_xk_y$  plane, on which the mirror Chern number is well-defined. The WCCs of  $k_x$ -directed Wilson loops in the  $k_z = 0$  plane are obtained in Fig. 2(h). The crossings and circles denote different  $m_z$  eigenvalues. The evolutions of the

WCCs indicate that mirror Chern numbers are  $C_{m_z}^\pm = \pm 2$ . Thus, we conclude that MSG1600  $\text{Mn}_3\text{ZnN}$  belongs to the MTCI phase.

## V. CONCLUSIONS

From the nonmagnetic TQC, we have constructed the CRs and MBRs for type-III and type-IV MSGs, which are consistent with the MTQC. Then we obtained the Fu-Kane-like formulas of SIs for MSGs directly by Smith decomposition. Next, we proposed an automatic process to search for magnetic topological materials, which is implemented in the online code TOPMAT to check CRs and compute SIs with the help of IRVSP. In the end, based on the DFT calculations, we found many magnetic topological candidates.

## ACKNOWLEDGMENTS

This work was supported by the National Natural Science Foundation of China (Grants No. 11974395 and No. 12188101), the Strategic Priority Research Program of Chinese Academy of Sciences (Grant No. XDB33000000), the China Postdoctoral Science Foundation funded project (Grant No. 2021M703461), and the Center for Materials Genome.

- 
- [1] K. V. Klitzing, G. Dorda, and M. Pepper, *Phys. Rev. Lett.* **45**, 494 (1980).
- [2] R. B. Laughlin, *Phys. Rev. Lett.* **50**, 1395 (1983).
- [3] D. C. Tsui, H. L. Stormer, and A. C. Gossard, *Phys. Rev. Lett.* **48**, 1559 (1982).
- [4] C. L. Kane and E. J. Mele, *Phys. Rev. Lett.* **95**, 226801 (2005).
- [5] B. A. Bernevig, T. L. Hughes, and S.-C. Zhang, *Science* **314**, 1757 (2006).
- [6] L. Fu, C. L. Kane, and E. J. Mele, *Phys. Rev. Lett.* **98**, 106803 (2007).
- [7] Y. Xia, D. Qian, D. Hsieh, L. Wray, A. Pal, H. Lin, A. Bansil, D. Grauer, Y. S. Hor, R. J. Cava *et al.*, *Nat. Phys.* **5**, 398 (2009).
- [8] H. Zhang, C.-X. Liu, X.-L. Qi, X. Dai, Z. Fang, and S.-C. Zhang, *Nat. Phys.* **5**, 438 (2009).
- [9] L. Fu, *Phys. Rev. Lett.* **106**, 106802 (2011).
- [10] T. H. Hsieh, H. Lin, J. Liu, W. Duan, A. Bansil, and L. Fu, *Nat. Commun.* **3**, 982 (2012).
- [11] Z. Wang, A. Alexandradinata, R. J. Cava, and B. A. Bernevig, *Nature (London)* **532**, 189 (2016).
- [12] J. Ma *et al.*, *Sci. Adv.* **3**, e1602415 (2017).
- [13] B. J. Wieder, B. Bradlyn, Z. Wang, J. Cano, Y. Kim, H.-S. D. Kim, A. M. Rappe, C. L. Kane, and B. A. Bernevig, *Science* **361**, 246 (2018).
- [14] F. Schindler, A. M. Cook, M. G. Vergniory, Z. Wang, S. S. P. Parkin, B. A. Bernevig, and T. Neupert, *Sci. Adv.* **4**, eaat0346 (2018).
- [15] X. Wan, A. M. Turner, A. Vishwanath, and S. Y. Savrasov, *Phys. Rev. B* **83**, 205101 (2011).
- [16] G. Xu, H. Weng, Z. Wang, X. Dai, and Z. Fang, *Phys. Rev. Lett.* **107**, 186806 (2011).
- [17] Z. Wang, H. Weng, Q. Wu, X. Dai, and Z. Fang, *Phys. Rev. B* **88**, 125427 (2013).
- [18] H. Weng, C. Fang, Z. Fang, B. A. Bernevig, and X. Dai, *Phys. Rev. X* **5**, 011029 (2015).
- [19] S.-Y. Xu, I. Belopolski, N. Alidoust, M. Neupane, G. Bian, C. Zhang, R. Sankar, G. Chang, Z. Yuan, C.-C. Lee *et al.*, *Science* **349**, 613 (2015).
- [20] B. Lv, N. Xu, H. Weng, J. Ma, P. Richard, X. Huang, L. Zhao, G. Chen, C. Matt, F. Bisti *et al.*, *Nat. Phys.* **11**, 724 (2015).
- [21] H. C. Po, A. Vishwanath, and H. Watanabe, *Nat. Commun.* **8**, 50 (2017).
- [22] E. Khalaf, H. C. Po, A. Vishwanath, and H. Watanabe, *Phys. Rev. X* **8**, 031070 (2018).
- [23] Z. Song, T. Zhang, Z. Fang, and C. Fang, *Nat. Commun.* **9**, 3530 (2018).
- [24] J. Kruthoff, J. de Boer, J. van Wezel, C. L. Kane, and R.-J. Slager, *Phys. Rev. X* **7**, 041069 (2017).
- [25] B. Bradlyn, L. Elcoro, J. Cano, M. Vergniory, Z. Wang, C. Felser, M. Aroyo, and B. A. Bernevig, *Nature (London)* **547**, 298 (2017).
- [26] F. Tang, H. C. Po, A. Vishwanath, and X. Wan, *Nature (London)* **566**, 486 (2019).
- [27] T. Zhang, Y. Jiang, Z. Song, H. Huang, Y. He, Z. Fang, H. Weng, and C. Fang, *Nature (London)* **566**, 475 (2019).
- [28] M. Vergniory, L. Elcoro, C. Felser, N. Regnault, B. A. Bernevig, and Z. Wang, *Nature (London)* **566**, 480 (2019).
- [29] R.-J. Slager, A. Mesaros, V. Juričić, and J. Zaanen, *Nat. Phys.* **9**, 98 (2013).
- [30] H. Watanabe, H. C. Po, and A. Vishwanath, *Sci. Adv.* **4**, eaat8685 (2018).

- [31] Y. Xu, L. Elcoro, Z.-D. Song, B. J. Wieder, M. Vergniory, N. Regnault, Y. Chen, C. Felser, and B. A. Bernevig, *Nature (London)* **586**, 702 (2020).
- [32] L. Elcoro, B. J. Wieder, Z. Song, Y. Xu, B. Bradlyn, and B. A. Bernevig, *Nat. Commun.* **12**, 5965 (2021).
- [33] B. Peng, Y. Jiang, Z. Fang, H. Weng, and C. Fang, *Phys. Rev. B* **105**, 235138 (2022).
- [34] A. Bouhon, G. F. Lange, and R.-J. Slager, *Phys. Rev. B* **103**, 245127 (2021).
- [35] G. F. Lange, A. Bouhon, and R.-J. Slager, *Phys. Rev. B* **103**, 195145 (2021).
- [36] [http://tm.iphy.ac.cn/TopMat\\_1651msg.html](http://tm.iphy.ac.cn/TopMat_1651msg.html).
- [37] J. Gao, Q. Wu, C. Persson, Z. Wang, *Comput. Phys. Comm.* **261**, 107760 (2021).
- [38] J. Gao, Y. Qian, H. Jia, Z. Guo, Z. Fang, M. Liu, H. Weng, and Z. Wang, *Sci. Bull.* **67**, 598 (2022).
- [39] Y. Xu, L. Elcoro, Z.-D. Song, M. Vergniory, C. Felser, S. S. Parkin, N. Regnault, J. L. Mañes, and B. A. Bernevig, [arXiv:2106.10276](https://arxiv.org/abs/2106.10276) (2021).
- [40] Y. Xu, L. Elcoro, G. Li, Z.-D. Song, N. Regnault, Q. Yang, Y. Sun, S. Parkin, C. Felser, and B. A. Bernevig, [arXiv:2111.02433](https://arxiv.org/abs/2111.02433) (2021).
- [41] G. Li, Y. Xu, Z. Song, Q. Yang, U. Gupta, Y. Sun, P. Sessi, S. S. Parkin, B. A. Bernevig, C. Felser *et al.*, [arXiv:2111.02435](https://arxiv.org/abs/2111.02435) (2021).
- [42] M. G. Vergniory, L. Elcoro, Z. Wang, J. Cano, C. Felser, M. I. Aroyo, B. A. Bernevig, and B. Bradlyn, *Phys. Rev. E* **96**, 023310 (2017).
- [43] L. Elcoro, B. Bradlyn, Z. Wang, M. G. Vergniory, J. Cano, C. Felser, B. A. Bernevig, D. Orobengoa, G. Flor, and M. I. Aroyo, *J. Appl. Crystallogr.* **50**, 1457 (2017).
- [44] M. I. Aroyo, D. Orobengoa, G. de la Flor, E. S. Tasci, J. M. Perez-Mato, and H. Wondratschek, *Acta Crystallogr. Sect. A* **70**, 126 (2014).
- [45] E. Tasci, G. de la Flor, D. Orobengoa, C. Capillas, J. Perez-Mato, and M. Aroyo, in *EPJ Web of Conferences* (EDP Sciences, 2012), Vol. 22, p. 00009.
- [46] J. F. Cornwell, *Group Theory in Physics* (Academic Press, United States, 1984), Vol. 1.
- [47] H.-W. Streitwolf, *Group Theory in Solid-state Physics* (The Book Service LTD, Great Bentley, England, 1971).
- [48] R.-X. Zhang and C.-X. Liu, *Phys. Rev. B* **91**, 115317 (2015).
- [49] See Supplemental Material at <http://link.aps.org/supplemental/10.1103/PhysRevB.106.035150>. for irreducible (co)representations of  $k$ -little groups, compatibility relations, magnetic band representations, and Fu-Kane-like symmetry indicators of all magnetic space groups.
- [50] W. Opechowski and R. Guccione, in *Magnetism*, edited by G. Rado and H. Suhl (Academic Press, New York, 1965), Vol. 2a, Chap. 3.
- [51] S. V. Gallego, E. S. Tasci, G. Flor, J. M. Perez-Mato, and M. I. Aroyo, *J. Appl. Crystallogr.* **45**, 1236 (2012).
- [52] Z.-D. Song, L. Elcoro, and B. A. Bernevig, *Science* **367**, 794 (2020).
- [53] L. Elcoro, Z. Song, and B. A. Bernevig, *Phys. Rev. B* **102**, 035110 (2020).
- [54] T. L. Hughes, E. Prodan, and B. A. Bernevig, *Phys. Rev. B* **83**, 245132 (2011).
- [55] S. Nie, Y. Sun, F. B. Prinz, Z. Wang, H. Weng, Z. Fang, and X. Dai, *Phys. Rev. Lett.* **124**, 076403 (2020).
- [56] J. Gao, Y. Qian, S. Nie, Z. Fang, H. Weng, and Z. Wang, *Sci. Bull.* **66**, 667 (2021).